

1 Accessing the Activation Mechanisms of Ethylene Photo- 2 Polymerization under Pressure by Transient Infrared Absorption 3 Spectroscopy

4 Sebastiano Romi, Samuele Fanetti,* and Roberto Bini



Cite This: <https://dx.doi.org/10.1021/acs.jpccb.0c06244>



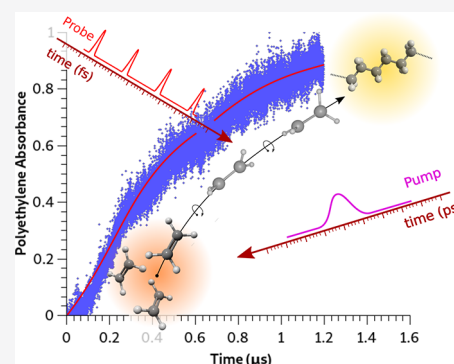
Read Online

ACCESS |

Metrics & More

Article Recommendations

5 **ABSTRACT:** The ambient temperature photoinduced polymerization of compressed
6 ($P < 1$ GPa) fluid ethylene was characterized by transient infrared absorption
7 spectroscopy with a resolution of few nanoseconds, 3 orders of magnitude higher than
8 previously reported. The reaction has been studied under both one- and two-photon
9 excitation evidencing in the latter case its occurrence only in the presence of different
10 transition metal oxides. Their photocatalytic activity is ascribed to the stabilization of
11 the excited biradicals through electron density exchange between the d orbitals of the
12 metal and the π antibonding orbitals of ethylene which lengthens the lifetime of the
13 biradicals. In both one- and two-photon activation cases the polymerization is
14 characterized by an initial step distinguished by a molecularity of 0.15 ± 0.02
15 identified as the activation step of the reaction lasting, in the one-photon excitation
16 case, a few hundreds of nanoseconds. Using pulsed excitation the reaction evolves
17 toward a free radical polymerization only under one-photon excitation whereas the
18 critical concentration of radicals required to propagate the reaction is never achieved in the two-photon excitation case. Comparison
19 with continuous wave excitation unambiguously identifies in the average power released to the sample the key factor to drive
20 quantitatively and qualitatively the polymerization.



1. INTRODUCTION

21 Pulsed laser techniques are central in providing detailed
22 information about the time evolution of chemical reactions in
23 condensed phases. These studies have been so far essentially
24 tackled in solution (see for example refs 1–3) whereas the
25 examples regarding chemical processes in crystals are extremely
26 limited.^{4,5} Between these two extremes lie the studies of pure
27 systems where the reaction leads to a phase change, whose
28 most enlightening examples are the polymerization reactions. A
29 quite large number of photopolymerizations have been treated
30 in different reviews with particular attention to the
31 determination of the rate constants of the different individual
32 steps which characterize the entire process.^{6,7} The principle
33 behind free-radical photopolymerizations is rather simple: a
34 short laser excitation pulse, generally in the ultraviolet (UV), is
35 absorbed by the monomer creating a suitable concentration of
36 free radicals to initiate the reaction. One of the first studies in
37 this field regards the ethylene polymerization initiated by a 248
38 nm laser pulse and characterized in a ms time scale with a few
39 μ s resolution.⁸ Besides the obvious importance for accessing
40 the dynamics of the early stages of the reactive process, the
41 relevance of this work is also related to the nature of the
42 polymer studied. Polyethylene (PE) is indeed the most
43 important synthetic polymer counting an incredible number
44 of diverse applications and to the fact that the synthesis is

conducted only with physical methods (light and pressure), an
important issue in terms of environmental impact. In this work
we succeeded in studying the first microsecond of the
photoinduced reaction, a temporal range never accessed before
and relevant to disclose the polymerization's initiation step
where the concentration of reactive precursors necessary to
propagate the reaction is built up.

The purely pressure induced polymerization of ethylene was
first studied in the compressed fluid: at 0.2 GPa and 453–523
K using spectroscopic methods to characterize the kinetics of
the reaction^{9,10} and at 2.3 GPa and 322 K.^{11,12} More recently,
the polymerization was induced also at ambient temperature in
the crystal phase using pressures in excess of 3 GPa by means
of a diamond anvil cell (DAC)¹³ and the P-T conditions of the
reaction threshold in the fluid phase fully characterized.¹⁴ The
instability boundary was found to decrease remarkably under
visible and near UV irradiation which induced a quantitative
transformation to a high quality crystalline polymer at ambient

Received: July 8, 2020

Published: August 26, 2020

63 temperature and pressures of a few kbar.¹⁵ The reaction was
64 demonstrated to occur following a two-photon excitation, a
65 quite surprising issue due to the low cross-section of such
66 transitions. The same approach was successfully applied to
67 scale the reaction to mm³ size samples.¹⁶

68 The efficiency of the photoinduced polymerization of
69 ethylene in compressed samples and the possibility of
70 exploring the effects of both one- and two-photon absorption
71 by tuning the excitation wavelength (250–500 nm) make of
72 ethylene a model system to investigate the reaction dynamics.
73 In addition, the access to the activation mechanisms of this
74 reaction is particularly intriguing in view of the remarkably
75 short lifetime of the excited species^{17–19} which barely agrees
76 with the efficiency of the process. We recently developed a
77 setup for transient infrared absorption experiments where
78 pump pulses of 30 ps produced by a parametric generator
79 (OPG) can be tuned from the IR to the UV, whereas the
80 sample evolution is probed by 200 fs IR pulses with an overall
81 time resolution better than 100 ps and the sample evolution
82 accessible up to hundreds ms delay. This setup allowed the
83 successful characterization of the superheating and homoge-
84 neous melting dynamics of ice crystals in a temporal interval
85 ranging from about 100 ps up to tens of ms after the energy
86 necessary for the melting was released to the crystal by a single
87 pump pulse.^{20,21} The characteristics of this setup are extremely
88 appealing to extend the study of the polymerization dynamics
89 of ethylene on a much shorter time scale than previously
90 accessed.⁸

91 Here we report a detailed characterization of the first
92 microsecond of the photopolymerization of fluid ethylene, at
93 room temperature and pressures lower than 1 GPa, induced by
94 both one- and two-photon electronic excitation. The reaction
95 kinetics under irradiation has been monitored allowing the
96 identification of the activation and propagation regimes which
97 are characterized by a different molecularity. In addition, we
98 demonstrated that the two-photon induced reactivity is
99 possible only when the reaction is catalyzed by metal oxides
100 through the stabilization of excited biradical species which act
101 as initiators.

2. EXPERIMENTAL SECTION

102 Membrane anvil cells equipped with grade 1 Diacell design
103 sapphires (from Almax-Easylab) with a culet of 950 μm have
104 been employed to compress fluid ethylene and studying in situ
105 the photoinduced reactivity. Cu–Be(2%) alloy gaskets were
106 used to laterally contain the samples. They were preindented
107 to a thickness of 30–60 μm and then drilled by spark erosion
108 to obtain a sample chamber of 450 μm of initial diameter and
109 eventually gilded when a non catalytic environment was
110 required.

111 Ethylene (99.5% from Sapio) was loaded in the sapphire
112 anvil cell by means of the spray-loading technique.²² The
113 pressure of the sample was calculated using the pressure shift
114 of a precalibrated ethylene infrared active C–H stretching
115 band as no gauge was used to avoid light-absorbing species
116 within the sample.

117 Different sources have been employed to photoinduce the
118 reaction depending on the experiment purpose. A cw xenon
119 lamp (Hamamatsu L10725) was used both for one- (260–400
120 nm) and two-photon (400–500 nm) excitation by filtering the
121 emission with appropriate short- and long-wavelength pass
122 filters. In both cases the light is focused on the sample by
123 means of a parabolic aluminum uncoated mirror with a

reflective focal length of 50.8 mm to a spot of comparable 124
dimensions of the sample diameter. The incident power was 125
measured by means of a power meter using the empty gasket 126
placed on the focal plane as diaphragm. For pulsed irradiations 127
and time resolved experiments we used as a pump a mode 128
locked Nd:YAG laser (EKSPLA PL2143A), giving a pulse 129
duration of 30 ps and an energy per pulse up to 25 mJ at 355 130
nm (third harmonic), with a repetition rate up to 10 Hz. This 131
wavelength was used for two-photon excitation, whereas in the 132
one-photon case the third harmonic was converted by an 133
optical parametric generator (EKSPLA PG401) into the visible 134
at 580 nm, and then frequency doubled by a BBO crystal ($6 \times$ 135
 $6 \times 7 \text{ mm}^3$, cut at 27° , from EKSMA) and selected by a UG11 136
filter to obtain a UV pulse at 290 nm. For all kind of pulsed 137
irradiation, the beam was attenuated at the desired energy by 138
means of reflective or absorbing neutral filters and focused on 139
the sample with a 200 mm uncoated quartz lens. The distance 140
between the sample and the lens is selected for every 141
experiment to obtain an homogeneous irradiation of the 142
sample chamber without hitting the gasket. The energy 143
released per pulse is measured after the transmission from 144
one sapphire by means of a calibrated Si-photodiode 145
(Hamamatsu S1722-02) and using the drilled gasket as a 146
diaphragm. The signal from the photodiode was read with a 2 147
GHz oscilloscope (Rohde & Schwarz RT2014) connected to a 148
computer and controlled through a Python3 software. 149

The transient IR measurements were performed with the 150
setup extensively described in refs 20 and 21 Briefly, a mode 151
locked Ti:sapphire oscillator, pumped with 3.7 W at 532 nm by 152
a doubled cw Nd:YAG laser source (OPUS 532, by Laser 153
Quantum), produces pulses at a repetition rate of 83 MHz 154
centered at $\sim 815 \text{ nm}$ with a fwhm of $\sim 35 \text{ nm}$ and a time 155
duration of $\sim 28 \text{ fs}$. By regenerative amplification (Pulsar, by 156
Amplitude Technology), using as a pump a Q-switched 157
Nd:YLF laser (YLF 621D, by B.M. Industries) with repetition 158
rate of 1 kHz, pulse duration of 120 ns and a power of $\sim 10 \text{ W}$, 159
an amplified beam at $\sim 820 \text{ nm}$ (1 kHz repetition rate, $\sim 0.5 \text{ mJ}$ 160
per pulse and time duration of 80–100 fs) is produced. This 161
beam is used to pump an optical parametric amplifier that 162
produces the probe and reference pulses peaked at 2880 cm^{-1} 163
with a fwhm of about 170 cm^{-1} and a total energy of about 2 164
 μJ per pulse. The reference pulse, produced using a $\sim 3\%$ 165
reflection from a CaF_2 window, is sent directly to the 166
revelation system whereas the transmitted beam is used as 167
probe. The probe beam is focused on the sample and 168
recollected with two gold coated 90° off-axis parabolic mirrors 169
with a focal length of 50.08 mm. The diameter of the probe 170
beam on the sample is about the half (200 μm) of the pump 171
pulse in order to probe the central part of it. Both probe and 172
reference are then focused with a 30° off-axis gold coated 173
parabolic mirror with a focal length of 108.9 mm on the slit of 174
a monochromator (Triax 180, by Horiba) equipped with a 100 175
grooves/mm ruled grating blazed at 6 μm , and detected with a 176
liquid nitrogen cooled MCT 32×2 array (InfraRed Associates 177
Inc.). The resulting resolution is $\sim 12 \text{ cm}^{-1}/\text{pixel}$, and the free 178
spectral range is about 380 cm^{-1} . One 32-element strip is 179
reserved for the probe, the other for the reference. The signal 180
from the detector is integrated by homemade electronics 181
capable to work at a repetition rate of 1 kHz, therefore on the 182
single pulse. The signal is digitized using a data acquisition 183
board (USB-1808G, by Measurement Computing with 18 bit 184
resolution and 0.2 MS/s sampling rate for channel) and 185
acquired by a computer using a real-time Linux kernel and a 186

187 Python3 homemade software. The single pulse absorbance is
 188 calculated as the base 10 logarithm of the ratio between the
 189 intensities measured for probe and reference. The neat
 190 absorbance of the product is then calculated as the mean
 191 absorbance value of the polyethylene at $2860\text{--}2880\text{ cm}^{-1}$,
 192 subtracted by the background value in the region below 2750
 193 cm^{-1} , where no absorbance of any species within the sample is
 194 present. The electronic synchronization realized between the
 195 pump/probe sources guarantees a time resolution in the order
 196 of 100 ps .²¹

197 Fourier transform infrared absorption spectra were measured
 198 with a Bruker-IFS 120 HR spectrometer suitably modified for
 199 experiments in diamond anvil cell, with an instrumental
 200 resolution set to 1 cm^{-1} .²³

201 The stainless steel powder used as a catalyst is AISI416 steel,
 202 the same steel used as a gasket in ref 15, while the Ti-based
 203 catalyst is $\text{Ti(IV)(MeO)}_4\cdot\text{H}_2\text{O}$ from Sigma-Aldrich with a
 204 purity of 95%.

3. RESULTS

205 As stated in the section 2, the region between 2860 and 2880
 206 cm^{-1} has been chosen to quantify the amount of polymer
 207 formed from our transient spectra (Figure 1). Only the C–H

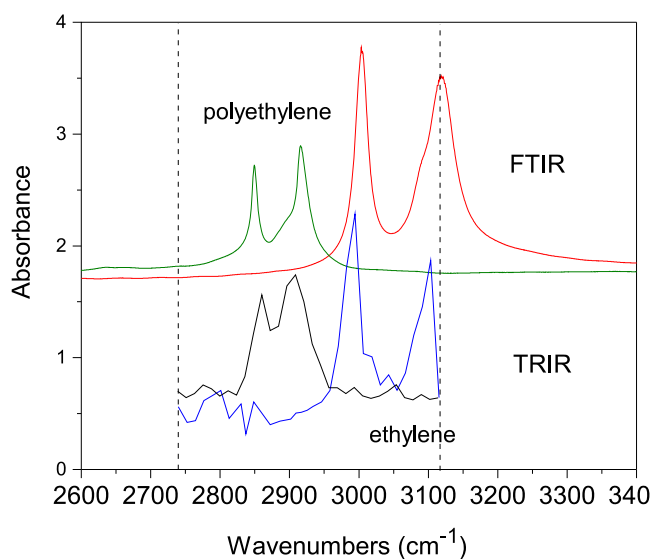


Figure 1. Comparison between the IR spectra of ethylene (blue and red traces) and polyethylene (black and green traces) measured using FTIR spectroscopy and transient infrared absorption spectroscopy (TRIR). The region included between the dashed lines ($2740\text{--}3115\text{ cm}^{-1}$) corresponds to the spectral width of the probe beam. In the TRIR spectra each pixel of the MCT array detector correspond to about 12 cm^{-1} . The first microsecond of the photo induced polymerization dynamics of ethylene has been characterized by using both one- and two-photon excitation and different metal catalysts in contact with the sample. For the sake of clarity we will present separately the results obtained with and without the catalysts. The polymerization has been followed by measuring the transient IR absorption spectrum in the region of the C–H stretching modes which undergo a remarkable change going from the monomer to the polymer because of the different hybridization of the carbon atoms. To quantify this issue and demonstrate the capability of our TRIR setup, we compare the spectra measured in pure ethylene and polyethylene samples contained in the sapphire anvil cell (SAC) by conventional FTIR spectroscopy and by averaging hundreds of single pulse transient spectra.

stretching modes involving saturated (sp^3) carbon atoms
 208 contribute to the absorption in this frequency range thus the
 209 absorbance change in this interval represents a reliable datum
 210 to be used in the kinetic analysis of the reaction. In the top
 211 panel of Figure 2, typical single pulse transient spectra
 212

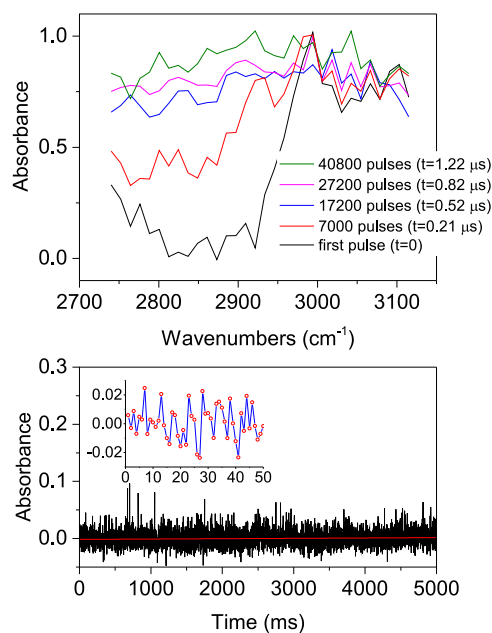


Figure 2. Upper panel: representative transient IR absorption spectra measured after the number of pump pulses reported in the legend were sent onto the sample. The conversion in irradiation time is also reported. The polymer formation is revealed by the progressive absorbance increase detectable between 2800 and 2900 cm^{-1} . Lower panel: evolution of the absorbance changes measured in the transient spectra between 2860 and 2880 cm^{-1} as a function of the probe delay after a single pump pulse was focused on the sample. The red line is the linear regression of these data characterized by a zero slope.

recorded after the reported number of pump pulses are
 213 shown, whereas in the lower panel we report that the time
 214 evolution of the polyethylene absorption after a single pump
 215 pulse (290 nm and $2\text{--}3\text{ }\mu\text{J}$) was focused onto the sample.
 216 Linear regression of these data clearly shows that we are not
 217 sensitive to the absorption changes induced by a single pump
 218 pulse. This result is not surprising if we consider that in ref 8
 219 the polyethylene's absorbance at 2857 cm^{-1} increased by less
 220 than 0.01 in 9 ms after a single pump pulse at 248 nm (10 ns
 221 duration and an energy of 250 mJ). Here, we are using pulses
 222 at higher wavelength (290 nm); the absorption is therefore
 223 characterized by a lower cross section, and in addition our
 224 pulses have a duration of 30 ps and energies of the order of 3
 225 μJ , resulting in a power of about 0.1 MW which is more than 2
 226 orders of magnitude smaller than that reported in ref 8. As a
 227 matter of fact, an absorbance change of 0.04 is detected only
 228 after having accumulated 1000 pump pulses therefore in
 229 perfect quantitative agreement with the results by Buback.⁸ As
 230 a result, our experimental apparatus cannot produce, with a
 231 single pump pulse, enough polyethylene to be detected
 232 independently of the delay of the probe pulse. In other
 233 words, we do not observe any change when the sample is not
 234 irradiated, i.e., the polymerization proceeds only under
 235 irradiation. The numbers of pump pulses multiplied by their
 236 duration represent therefore the temporal coordinate of our
 237

238 process, and it will be used in the following to interpret the
239 kinetic data.

240 **3.1. Reaction in the Absence of Metal Catalysts.** With
241 the absence of metal catalysts, we mean that in all of these
242 experiments we avoided the contact of fluid ethylene with the
243 metal gasket employed for confining the sample and with the
244 possible derived compounds, as for example oxides. This was
245 achieved by protecting the Cu–Be gaskets with gold that, as it
246 will be shown in the following, does not exhibit any catalytic
247 activity in these conditions. An excitation wavelength ranging
248 from 286 to 290 nm was employed to one-photon excite the
249 monomer to the symmetry allowed $1B_{1u}$ state ($\pi\pi^*$) which is
250 extremely broad and centered at ambient conditions at 7.66 eV
251 (~ 162 nm).²⁴ This absorption overlaps sharper absorption
252 bands relative to the transition to the $1B_{3u}$ state which has
253 Rydberg character ($\pi,3s$). After each pump pulse, with an
254 energy of 2.6 μJ , we acquired and averaged from 300 to 500
255 transient spectra each one measured with a single probe pulse,
256 in order to improve the signal-to-noise ratio. The absorbance
257 variation detected in the averaged spectra between 2860 and
258 2880 cm^{-1} is reported as a function of the irradiation time in
259 Figure 3. The time scale is obtained by multiplying the number

the monomer took place in this time interval. The kinetics, 267
exhibiting a sigmoidal shape as expected for an activated 268
process, presents an inflection point after about 0.15 μs and a 269
clear slope decrease after about 0.3 μs . The curve has been 270
reproduced using the Avrami model formerly developed to 271
describe the crystal growth from the melt^{25–27} and then 272
extended to the study of solid-state reactions controlled by 273
diffusion.²⁸ The amount of PE formed as a function of time is 274
described by the relation: 275

$$I(t) = I_{\infty}(1 - e^{[-k(t-t_0)^n]}) \quad (1) \quad 276$$

where I_{∞} is the intensity of the PE absorption at the end of the 277
reaction ($t = \infty$), t_0 is the reaction starting time, $k^{1/n}$ is the rate 278
constant, and n is a parameter related to the dimensionality of 279
the growth process. The fit parameters are reported as an inset 280
in Figure 3. The t_0 value of 25 ns is mainly related to our 281
sensitivity in detecting a minimum amount of polymer, 282
whereas the n value of 1.2 indicates that an overall linear 283
growth of the polymer, the absence of branching, takes place. 284

When gold rings were used to prevent the contact with the 285
gasket metal, and its possible catalytic effect, we did not detect 286
any reactivity once the sample was irradiated with laser pulses 287
at 355 nm and power up to 25 μJ which, accordingly to our 288
previous experiments,¹⁵ should be extremely efficient in 289
triggering the reaction between 0.2 and 0.8 GPa through 290
two-photon absorption processes. A further confirmation of 291
the sample stability to irradiation with wavelengths out of one- 292
photon resonance was gained by the missed observation of 293
reactivity when the sample was irradiated by a Xe lamp (400– 294
500 nm) which guaranteed a much higher power (45–160 295
mW and a duration 1–2 h) released to the sample. The 296
difference with the results obtained in ref 15 is ascribed to the 297
catalytic effect of the stainless-steel gasket which was, in that 298
case, in contact with the sample, making it mandatory to 299
explore the reactivity in the presence of catalytic materials. 300

3.2. Reaction in the Presence of Metal Catalysts. Two- 301
photon induced polymerization was instead observed when the 302
sample was in contact with different metallic compounds 303
sharply demonstrating its occurrence only in the presence of 304
catalysts. In one case we just avoided the gasket gilding leaving 305
the copper–beryllium alloy (2% in Be) gasket in contact with 306
the sample. In other two experiments we used gilded gaskets 307
adding to the sample a very small amount of fine powdered 308
titanium(IV) methoxide $\text{Ti}(\text{OCH}_3)_4$ in one case, and stainless 309
steel in another. With two of the three catalysts we irradiated 310
fluid ethylene compressed at 0.2 GPa, Cu–Be, and 0.7 GPa, 311
 $\text{Ti}(\text{OCH}_3)_4$, with 25 μJ per pulse of the third harmonic (355 312
nm) of the Nd:YAG laser source, a wavelength that can only 313
be absorbed by ethylene through a two-photon process.^{15,29,30} 314
In these cases, we did not measure the transient spectra but we 315
just checked the occurrence of the reaction by measuring FTIR 316
absorption spectra. In the two experiments where stainless 317
steel powder was added to the sample we measured two 318
kinetics using the transient absorption technique with the same 319
pump wavelength and 20 and 40 μJ per pulse, respectively. In 320
Figure 4 we report some of the IR absorption spectra measured 321
in the first two experiments and those obtained after the 322
completion of the kinetic studies performed in the presence of 323
stainless steel. Contrary to the observation made in the 324
absence of catalysts, we observe, as a consequence of 325
irradiation, the appearance of the characteristic C–H 326
stretching bands of the polymer below 3000 cm^{-1} . The 327
reaction is also rather efficient in agreement with previous 328

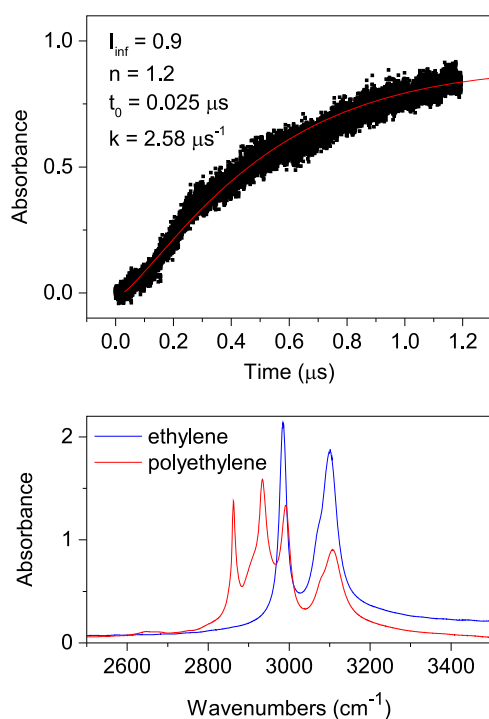


Figure 3. Reactivity induced by one-photon excitation with pulsed laser radiation (30 ps; 2.6 μJ) at 290 nm. Upper panel: absorption of the polymer bands as a function of irradiation time as obtained by the transient spectra. The red line is the fit of these data according to the Avrami's model (eq 1), the parameters used in the fit are reported as an inset. Lower panel: comparison of the FTIR spectra measured before starting the irradiation (blue trace) and after its completion (red trace).

260 of pump pulses by their duration (30 ps) that it is possible, as
261 mentioned before, in view of the missing reaction's evolution
262 with time after a single pump pulse. This graph is therefore the
263 kinetic curve of the photoreaction measured in the first 1.2 μs .
264 In the same figure we also report the comparison of the IR
265 spectra measured by FTIR spectroscopy before and at the end
266 of the irradiation, showing that a conversion of about 53% of

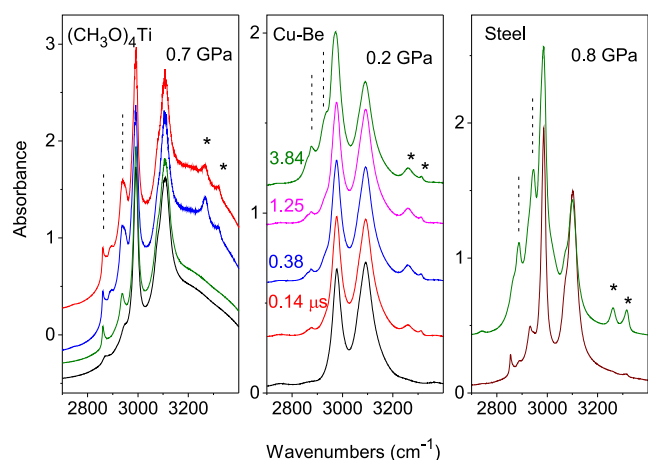


Figure 4. FTIR spectra measured in the C–H stretching region during and after the two-photon induced reaction using 355 nm laser pulses in the presence of different metal catalysts. Dashed lines mark the position of the polymer C–H stretching bands, and asterisks mark the bands assigned to C–H stretching involving carbon atoms with sp hybridization. Left: evolution of the spectrum in the presence of titanium methoxide. The green trace is obtained after 20 min of irradiation with cw light (400–500 nm and 160 mW) from a Xe lamp; the blue trace after 1 μ s of irradiation with pulses having an energy of 20 μ J (36 000 pulses) and the red one after 24 h without irradiation. Center: evolution of the spectrum with the irradiation time with uncoated Cu–Be gasket, pulses of 25 μ J at 355 nm have been employed, and the times reported in the figure correspond to the number of pulses multiplied by their duration (30 ps). Right: final spectra obtained after the end of the kinetic studies performed using pulses of 20 μ J (red trace) and 40 μ J (green trace) in the presence of stainless steel powder.

cw light (see Figure 4), both from a laser source or a lamp, in agreement with the findings reported in ref 15.

The two-photon induced polymerization kinetics was studied by transient IR absorption spectroscopy in samples containing stainless steel powder at a pressure of 0.8 GPa. Two different experiments were performed irradiating the sample with laser pulses at 355 nm and energies of 20 and 40 μ J per pulse, respectively. As already reported for the one-photon experiments, we averaged 300–500 transient spectra for every pump pulse obtaining the reaction evolution reported in Figure 5. Also in this case we report the data using a time scale

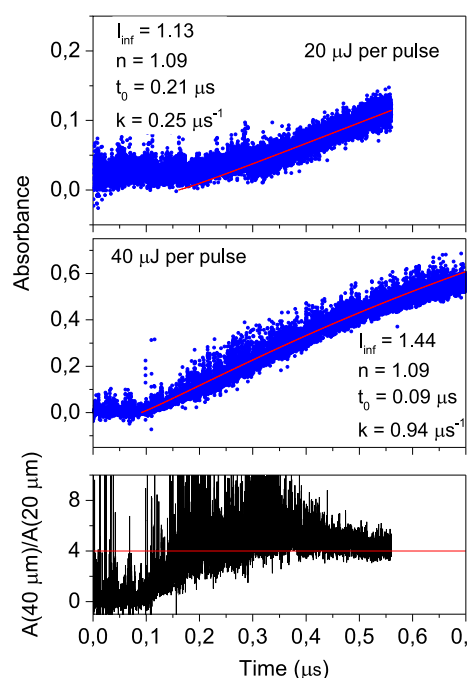


Figure 5. Upper panels: kinetics of the two-photon induced reaction with 20 (top) and 40 (middle) μ J per pulse at 355 nm. In both panels the fit parameters according to the Avrami eq (eq 1) are also reported. Lower panel: evolution of the ratio between polymer absorbances measured in the two kinetics: as the energy per pulse ratio is 2, an absorbance ratio equal to 2 is expected for a linear dependence on the incident power (one-photon absorption), whereas a ratio equal to 4 indicates a quadratic dependence and thus a two-photon absorption process.

obtained by multiplying the number of pump pulses for their duration (30 ps) because the reaction proceeds only under irradiation.

The two sets of data were reproduced by using the Avrami model (eq 1) fixing the I_{∞} parameter to the expected PE absorbance assuming the complete ethylene transformation with the datum obtained by using the FTIR spectra measured at the end of the experiments (these spectra are reported in the right panel of Figure 4). In reproducing the two kinetics, we used in both cases the same n value of 1.09, which indicates a linear growth of the polymer. An almost double induction time t_0 is measured in the experiment performed with the lower pulse energy, in which also the rate constant is about four times smaller than in the 40 μ J experiment. This ratio between the rate constant values is that expected for a two-photon activation process since the amount of excited ethylene molecules, which is in first approximation equal to the number of active species, shall scale with the square of the incident

report,¹⁵ leading to a conversion of about 20% of the monomer for supplied energies of about 3 and 1 J when the reaction is catalyzed by Cu–Be and $\text{Ti}(\text{OCH}_3)_4$, respectively. The comparison of these results are extremely qualitative because of the different pressures where the two experiments have been performed.

The infrared spectra of the polymer obtained by two-photon irradiation are worth investigating further. The asymmetric and symmetric $-\text{CH}_2$ stretching give rise to two bands, at about 2925 and 2855 cm^{-1} , respectively, which characterize the spectra of PE. A third band of weaker intensity forms between these two bands at about 2895 cm^{-1} , and this band can be assigned to the symmetric stretching of the $-\text{CH}_3$ group, whereas the band corresponding to the asymmetric stretching of this group appears as a shoulder on the high frequency side of the corresponding band relative to the $-\text{CH}_2$ groups. The spectral signatures of $-\text{CH}_3$ groups suggests the presence of a large number of terminations. Another peculiar feature present in all of the spectra of the polymers obtained in these catalyzed two-photon reactions is the presence of two bands at 3263(3) and 3315(3) cm^{-1} . These are unambiguously assigned to C–H stretching modes of sp hybridized carbon atoms representing therefore or chain terminations or byproducts of the polymerization reaction. As can be seen in the case of the reaction catalyzed by titanium methoxide the intensity of these two bands decreases with time (53% in 24 h) when the sample is not irradiated (see Figure 4), thus suggesting their metastable character. Another interesting observation is that these bands appear only when ethylene is irradiated with pulsed laser light but are not present in samples irradiated by

power. This is clearly shown in the lower panel of Figure 5 where we report the ratio between the polymer absorbance in the two experiments as a function of time. As it can be seen the quadratic dependence on the incident power is perfectly satisfied in the time range where both reactions proceed. Finally, as already observed in the other two-photon induced catalyzed reactions, absorption bands that can be assigned to C–H modes involving sp carbon atoms also form in this case. Interestingly, the intensity ratio between these bands measured in the two experiments, 20 and 40 μJ , is much higher (~ 10 times) than expected for a two-photon process (~ 4 times) suggesting their possible origin by a higher order absorption process.

3.3. Reactions Molecularity. We can gain further information about the mechanisms characterizing the very first instants of the photoinduced reaction by studying the molecularity of the process and its possible evolution with time. This information is crucial for the identification of the number of species characterizing the different reaction steps. To this purpose we used the simple kinetic relation^{9,14}

$$\nu = k[\text{Csp}^2]^m \quad (2)$$

where the reaction rate ν is related to the ethylene concentration through the rate constant k and the process' molecularity m . Since our detection window was centered on the frequency of the C–H stretching of the polymer we could not reliably detect the ethylene absorption bands. For this reason instead of the monomer concentration we follow that of sp³ carbon atoms whose increase in time is proportional (K_p), because of the different absorption cross-section, to the ethylene concentration decrease. The above kinetic law is usually analyzed through the log–log relation which taking into account the use of the polymer concentration becomes

$$\log(\nu) = m\log[\text{Csp}^3] + \log(k) + \log(K_p) \quad (3)$$

We fitted the time evolution of the polymer concentration using a stretched exponential to have an analytical function for calculating at any time the corresponding reaction rate value. In Figure 6 we report the log–log plot for the reaction induced

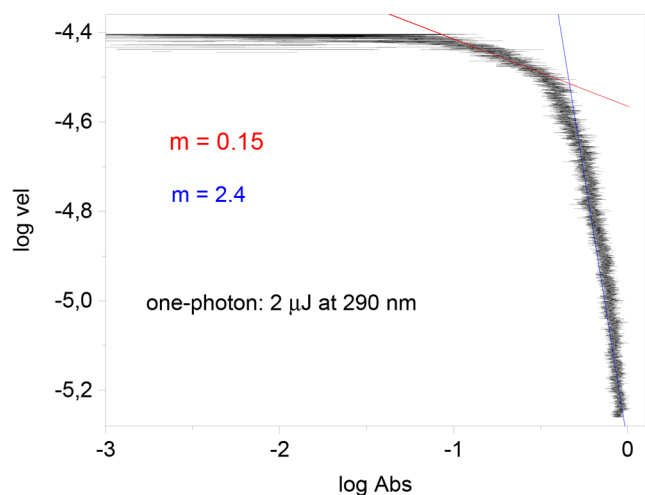


Figure 6. log–log plot of the reaction rate vs the absorbance (concentration) of polyethylene for the one-photon induced reaction. The two linear fit indicate the reaction steps characterized by a consistent change of the molecularity value.

by one-photon absorption of 2 μJ pulses at 290 nm. As it is evident from the figure, at least two different regimes are identified with a remarkably different value of the molecularity. The early reaction stage is characterized by a molecularity of 0.15 which becomes 2.4 after about 0.3 μs from the reaction beginning, a time corresponding to the slope change detected in the kinetic curve (see Figure 3).

The same analysis has also been performed for the two-photon induced reaction using stainless steel in contact with the sample and laser pulses of 20 and 40 μJ . The corresponding log–log plots are reported in Figure 7. Contrary to what we

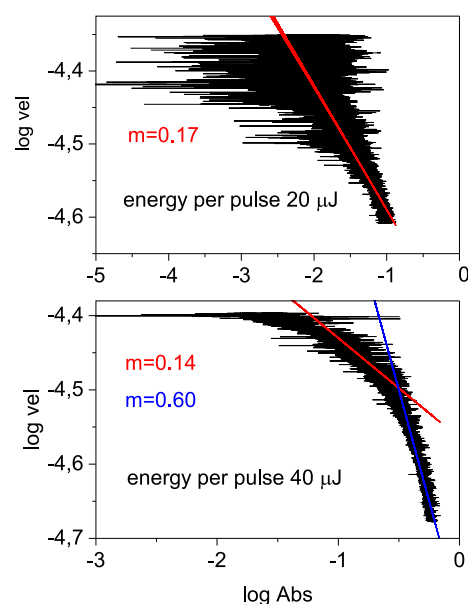


Figure 7. log–log plot of the reaction rate vs the absorbance (concentration) of polyethylene for the two-photon induced reaction. Upper panel: reaction induced by 20 μJ laser pulses (355 nm) exhibiting a single molecularity regime. Lower panel: reaction induced by 40 μJ laser pulses (355 nm) where two regimes characterized by different molecularity values can be identified.

observe in the one-photon excitation case, the two-step regime is observed only in the reaction performed with higher energy pulses. The molecularity of the initial reaction step is nearly identical in both experiments, also nicely agreeing with that characterizing the analogous step in the one-photon reaction. This step is likely the only probed in the reaction performed with 20 μJ per pulse because of the very limited amount of polymerized monomer. Where the higher energy pulse experiment is concerned, a slope (molecularity) change is observed after about 0.45 μs but the extent of the molecularity change is not as large as observed in the one-photon experiments changing only from 0.14 to 0.6.

4. DISCUSSION

The free radical polymerization of ethylene can be triggered by absorption of light resonant with the transition to the valence $\pi\pi^*$ excited state ($1B_{1u}$). This transition, one-photon symmetry allowed and characterized by an oscillator strength of 0.34, appears as a broad band peaked at 7.66 eV (~ 162 nm) and extending to the red up to 215 nm at ambient conditions in low pressure gas phase.³¹ Superimposed to this broad absorption are observed sharper bands related to the transition to the Rydberg ($\pi,3s$) state with origin at 7.11 eV (~ 175 eV

457 nm).^{24,31} Ethylene undergoes an enormous structural change
458 upon excitation to the $\pi\pi^*$ excited state consisting in a 90°
459 relative twisting of the CH_2 groups and the consequent
460 formation of a biradical³² with the carbon atoms described by a
461 sp^3 -like hybridization and a C–C bond length which is
462 estimated in the 1.38–1.47 Å range.^{33,34} The same effect, i.e.,
463 the formation of biradicals able to trigger the polymerization
464 reaction, is also achieved by using two-photon excitation.¹⁵
465 The excited state reached by absorption of two photons at 350
466 nm is presumably the same $\pi\pi^*$ state reached by one-photon
467 absorption. This transition is two-photon forbidden, but it
468 could be activated by vibronic coupling or by virtue of the
469 molecular symmetry change which relaxes the selection rules.
470 It should be mentioned that an alternative assignment,
471 proposing the final state as the $\pi,3s$ Rydberg state,^{29,30} is
472 barely compatible with the changes observed upon compression.
473 According to the low cross-section of the two-photon
474 transition, the polymerization reaction initiation is therefore
475 related to the interaction of the excited biradical with a ground
476 state ethylene molecule. However, the excited molecule relaxes
477 to the ground state through conical intersections thus reducing
478 the lifetime of the valence state to a few (20 ± 10)
479 femtoseconds.^{17–19} The extremely fast relaxation, 1–2 orders
480 of magnitude shorter than the collision frequency calculated at
481 the density conditions of the reaction, raised doubts about the
482 effective primary role of the excited biradical in the reaction
483 activation.¹⁵

484 The first remarkable result of this study is to shed light on
485 this issue. In fact, we demonstrated that the polymerization can
486 be two-photon induced only in the presence of a metal catalyst
487 or better of a metallic ion. When the sample is contained by
488 gilded gaskets, we do not observe any two-photon induced
489 reactivity both with cw and pulsed laser light. On the contrary,
490 the reaction is observed when metal gaskets (Cu–Be and
491 stainless steel) are employed or when a few amount of
492 titanium(IV) methoxide or stainless steel powder is put into
493 the sample. The catalytic activity is ascribable to the presence
494 of the oxides of these transition metals which are always
495 present on their surface. As a matter of fact, the missed
496 observation of the reaction with gold is an indirect proof of the
497 oxides activity, since gold is extremely inert to oxidation at the
498 sample loading conditions. On the contrary the reaction is
499 observed in any condition, including with the sample in
500 contact only with gold, when it is induced by one-photon
501 absorption. This is not surprising since the two processes, one-
502 and two-photon absorption, are characterized by cross sections
503 that differ by several orders of magnitude. This means that the
504 number, i.e., the concentration, of excited molecules is
505 sufficiently large in the reaction triggered by one-photon
506 absorption to guarantee the propagation of the reaction likely
507 also by means of the direct reaction between two biradical
508 species. The initiation and propagation steps of the one-
509 photon induced reaction are perfectly identified and quantified
510 by the log–log plot reported in Figure 6. The early stage of the
511 reaction presents a molecularity lower than 1 (0.15), a value
512 indicating that most of the reactive species prepared through
513 the excitation “relax” to the ground state molecular structure
514 without reacting. This stage can be identified as a kind of
515 activation step. After about $0.3 \mu\text{s}$ the concentration of reactive
516 species is such to guarantee a molecularity ≥ 2 which is the
517 minimum value expected for the polymerization reaction. The
518 value found here, 2.4, is in excellent agreement with those
519 found by Buback at comparable reaction pressures both in the

photoinduced⁸ (2.0) and in the thermal⁹ (2.5) polymerization
520 reactions. The time window where the regime change occurs
521 obviously depends on the incident power, i.e., the concen-
522 tration of reactive initiators, but for the first time this initiation
523 step is identified and quantified in a few hundreds of ns. One
524 aspect worth highlighting regards the time ($0.3 \mu\text{s}$) where we
525 observe the sudden molecularity change, in fact although a
526 clear slope decrease is detected at the same delay in the kinetic
527 curve (see Figure 3), no interpretation of this feature can be
528 provided by the Avrami’s model. 529

It is interesting at this stage to compare these findings with
530 the molecularity data obtained in the two-photon induced
531 reaction (see Figure 7). A clear difference is noted for the two
532 incident powers used: a single regime characterized by a
533 molecularity of 0.17 is observed in the entire time window
534 ($0.55 \mu\text{s}$) investigated when energy laser pulses of $20 \mu\text{J}$ were
535 used, whereas when a double energy per pulse is employed we
536 observe, as in the one-photon case, two regimes: the first
537 characterized by a molecularity of 0.14 increasing also in this
538 case after about $0.3 \mu\text{s}$ to 0.6. The comparison with the one-
539 photon findings unambiguously confirms a preliminary
540 activation step common to all the kinetics characterized by a
541 molecularity ranging between 0.14 and 0.17 and exhibiting a
542 different duration depending on the concentration of initiators
543 (excited biradicals). This step is the only detected in the two-
544 photon induced reaction with pulses of $20 \mu\text{J}$ where the critical
545 concentration of reactive species requested to propagate the
546 reaction is likely never reached, at least in the time window
547 investigated. By doubling the power we have indications of a
548 change in the mechanism but without reaching molecularity
549 values characteristic of the reaction propagation. 550

As we clearly demonstrated the two-photon induced
551 reaction is catalyzed by transition metals ions. Recently Cr^{VI} ,
552 in the form of monochromate supported on silica, has been
553 used as photocatalysts to trigger the ethylene polymerization at
554 room temperature in the gas phase.³⁵ The suggested two-step
555 mechanism envisages the Cr^{VI} reduction by presumably excited
556 ethylene molecules and the successive polymerization. The
557 formation of ethylene-metal complexes is rather well
558 established to occur through the donation and possible back-
559 donation of electron density between the d orbitals of the
560 metal ion and the π and π^* molecular orbitals of ethylene.³⁶
561 The interaction between ground state ethylene and different
562 metal cations was studied by DFT calculations showing that
563 the main contribution to the covalent term stems from the σ
564 donor part, whereas the back-donation (π) acceptor bonding is
565 less important.³⁷ However, in the present case, the stabilization
566 of the biradical is of interest, i.e., of the excited molecule whose
567 lifetime is normally too short for trigger efficiently the
568 reactivity. The formation of biradical states through electronic
569 charge transfer in complexes between excited S_1 ethylene and
570 metals has been studied by ab initio calculations in the case of
571 Ca atoms.³⁸ The formation of a rather stable complex having
572 the biradical geometry where the Ca atom anchors to the two
573 carbons through the bond formed from the d_{xy} orbital of Ca
574 and π^* orbital of ethylene was demonstrated. Assuming an
575 analogous stabilization of the biradical species, a concentration
576 large enough to make possible reactive collisions with ground
577 state ethylene molecules or already formed oligomers can be
578 envisaged. As a matter of fact, the almost linear growth of the
579 polymer is fully supported by the kinetic analysis with the
580 Avrami’s model, which always supports through the dimen- 581

582 sional n parameter a linear growth of the product in a diffusion
583 controlled reaction.

584 The last comment regards the differences observed between
585 the reaction induced by two-photon absorption with cw or
586 pulsed sources. In the first case, cw lasers or lamps, we fully
587 confirm the results of ref 15 obtaining a complete trans-
588 formation of the monomer to a high quality crystalline
589 polyethylene, notwithstanding that the reaction occurs through
590 the catalytic action of the metal gasket as extensively discussed
591 above. When pulsed laser sources (30 ps) are used the reaction
592 is remarkably slower, partial and moreover the formation of
593 acetylenic moieties and methyl groups is observed especially in
594 the two-photon experiments (20–40 μJ per pulse) suggesting
595 the presence of a larger amount of terminations (shorter
596 oligomers). In addition, the amount of sp carbon atoms
597 spontaneously decreases with time when the sample is not
598 irradiated thus indicating that the triple bonds belong to
599 metastable byproducts. Due to the remarkable reproducibility
600 of these findings, we ascribe this diversity to the nature of the
601 light field employed. The laser pulses used in this work are
602 characterized by peak powers of the order of 1 MW but
603 average power of the order of 10^{-1} mW and, therefore, 3
604 orders of magnitude smaller than the one characterizing cw
605 experiments. The average power appears therefore as the key
606 parameter in preparing and maintaining a concentration of
607 initiators sufficient for propagating the polymerization reaction.
608 On the other side, a high peak power is the prerequisite for
609 inducing non linear optical phenomena, as in this case can be
610 multiphoton absorption to the diffuse Rydberg states,³¹ which
611 can lead to the deprotonation of the monomer and the
612 consequent formation of an acetylenic species. The latter
613 statement is also supported by the strongly nonlinear
614 dependence on the incident power of the formation of sp
615 species in the stainless steel catalyzed reaction.

5. CONCLUSIONS

616 The photopolymerization of ethylene induced by one- and
617 two-photon excitation has been characterized in the fluid phase
618 for pressures below 1 GPa. The outcome of this study is 2-fold
619 contributing to considerably deepen our fundamental knowl-
620 edge of this reaction. The most important and innovative result
621 concerns the characterization of the reaction's first micro-
622 second by time-resolved transient infrared absorption experi-
623 ments with a few ns resolution. Thanks to this careful sampling
624 of the photopolymerization dynamics we identified the
625 activation step of the reaction, characterized by a molecularity
626 of 0.15 ± 0.02 , and a temporal extension dependent on the
627 concentration of excited ethylene biradicals that on turn results
628 from the incident power and the transition cross-section. In
629 one-photon induced reactions after 300 ns, the activation step
630 is replaced by a molecularity increase to more than 2, as
631 expected for the free radical propagation reaction. This is
632 instead never observed in the two-photon induced reactions
633 where the critical concentration for triggering the propagation
634 step is evidently never reached because of the much lower
635 cross-section. The second important result of this study is the
636 recognition of the catalytic role played by the metal gaskets in
637 triggering the two-photon induced polymerization, a general
638 and critical issue in many studies conducted at high pressure in
639 the presence of laser light. The reduced concentration of
640 excited molecules and their ultrafast relaxation to the ground
641 state prevent the reactivity unless the excited biradicals are
642 stabilized by the interaction with different metallic ions (Ti, Fe,

and Cu). This stabilization, corresponding to a lengthening of 643
the biradical lifetime, likely occurs through the electronic 644
interaction between the d orbitals of the metal ion and the π^* 645
molecular orbitals of ethylene. Finally, as the quality of the 646
polymer resulting from the photoinduced reaction is 647
concerned it appears that cw irradiation allows the attainment 648
of a reduced amount of defects and chain terminations, and 649
then a much better crystallinity, with respect to pulsed 650
irradiation. The latter, characterized by high peak power, can 651
favor the molecule photodissociation through the transition to 652
Rydberg states by means of multiphoton absorption processes 653
with the consequent formation of methylic and acetylenic 654
groups. 655

AUTHOR INFORMATION

Corresponding Author

Samuele Fanetti – LENS, European Laboratory for Non-linear
Spectroscopy, I-50019 Sesto Fiorentino, Firenze, Italy; Istituto di
Chimica dei Composti OrganoMetallici, ICCOM, I-50019
Sesto Fiorentino, Firenze, Italy; orcid.org/0000-0002-5688-6272; Email: fanetti@lens.unifi.it

Authors

Sebastiano Romi – LENS, European Laboratory for Non-linear
Spectroscopy, I-50019 Sesto Fiorentino, Firenze, Italy

Roberto Bini – LENS, European Laboratory for Non-linear
Spectroscopy, I-50019 Sesto Fiorentino, Firenze, Italy; Istituto di
Chimica dei Composti OrganoMetallici, ICCOM, I-50019
Sesto Fiorentino, Firenze, Italy; Dipartimento di Chimica "Ugo
Schiff", Università di Firenze, I-50019 Sesto Fiorentino, Italy;
orcid.org/0000-0002-6746-696X

Complete contact information is available at:

<https://pubs.acs.org/10.1021/acs.jpccb.0c06244>

Notes

The authors declare no competing financial interest.

ACKNOWLEDGMENTS

We thank the European Laboratory for Nonlinear Spectros-
copy (LENS) for hosting the research, the Deep Carbon
Observatory, and the "Fondazione CR Firenze" for strong
support. The research has been supported by the following
grants: "The Extreme Physics and Chemistry Community of
the Deep Carbon Observatory" funded by the Alfred P. Sloan
Foundation and "Dinamiche di fusione di ghiacci e idrati:
accesso al regime mesoscopico" funded by Fondazione Cassa
di Risparmio di Firenze. We also thank MIUR-Italy ("Progetto
Dipartimenti di Eccellenza 2018-2022" allocated to Depart-
ment of Chemistry "Ugo Schiff").

REFERENCES

- (1) Rosspeintner, A.; Lang, B.; Vauthey, E. Ultrafast Photochemistry
in Liquids. *Annu. Rev. Phys. Chem.* **2013**, *64*, 247–271.
- (2) Carpenter, B. K.; Harvey, J. N.; Orr-Ewing, A. J. The Study of
Reactive Intermediates in Condensed Phases. *J. Am. Chem. Soc.* **2016**,
138, 4695–4705.
- (3) Orr-Ewing, A. J. Taking the Plunge: Chemical Reaction
Dynamics in Liquids. *Chem. Soc. Rev.* **2017**, *46*, 7597–7614.
- (4) Poulin, P. R.; Nelson, K. A. Irreversible Organic Crystalline
Chemistry Monitored in Real Time. *Science* **2006**, *313*, 1756–1760.
- (5) Xian, R.; Corthey, G.; Rogers, D. M.; Morrison, C. A.;
Prokhorenko, V. I.; Hayes, S. A.; Miller, R. J. D. Coherent Ultrafast
Lattice-Directed Reaction Dynamics of Triiodide Anion Photo-
dissociation. *Nat. Chem.* **2017**, *9*, 516–522.

- (6) Beuermann, S.; Buback, M. Rate Coefficients of Free-Radical Polymerization Deduced from Pulsed Laser Experiments. *Prog. Polym. Sci.* **2002**, *27*, 191–254.
- (7) Barner-Kowollik, C.; Russell, G. T. Chain-Length-Dependent Termination in Radical Polymerization: Subtle Revolution in Tackling a Long-Standing Challenge. *Prog. Polym. Sci.* **2009**, *34*, 1211–1259.
- (8) Buback, M.; Hippler, H.; Schweer, J.; Vogeles, H.-P. Time-Resolved Study of Laser-Induced High Pressure Ethylene Polymerization. *Makromol. Chem., Rapid Commun.* **1986**, *7*, 261–265.
- (9) Buback, M. The High Pressure Polymerization of Pure Ethylene. *Makromol. Chem.* **1980**, *181*, 373–382.
- (10) Buback, M. Spectroscopic Investigation of the High Pressure Ethylene Polymerization. *Z. Naturforsch., A: Phys. Sci.* **1984**, *39*, 399–411.
- (11) Wieldraaijer, H.; Schouten, J. A.; Trappeniers, N. J. Investigation of the Phase Diagrams of Ethane, Ethylene, and Methane at High Pressures. *High Temp. - High Press.* **1983**, *15*, 87–92.
- (12) Van der Putten, L.; Schouten, J. A.; Trappeniers, N. J. A differential Scanning Calorimetry Study of Ethylene and Propane up to 10 kbar: the Phase Diagram of Ethylene up to 23 kbar. *High Temp. - High Press.* **1986**, *18*, 255–264.
- (13) Chelazzi, D.; Ceppatelli, M.; Santoro, M.; Bini, R.; Schettino, V. Pressure-Induced Polymerization in Solid Ethylene. *J. Phys. Chem. B* **2005**, *109*, 21658–21663.
- (14) Scelta, D.; Ceppatelli, M.; Bini, R. Pressure Induced Polymerization of Fluid Ethylene. *J. Chem. Phys.* **2016**, *145*, 164504.
- (15) Chelazzi, D.; Ceppatelli, M.; Santoro, M.; Bini, R.; Schettino, V. High-pressure Synthesis of Crystalline Polyethylene Using Optical Catalysis. *Nat. Mater.* **2004**, *3*, 470–475.
- (16) Ceppatelli, M.; Bini, R. Light-Induced Catalyst and Solvent-Free High Pressure Synthesis of High Density Polyethylene at Ambient Temperature. *Macromol. Rapid Commun.* **2014**, *35*, 787–793.
- (17) Mestdag, J. M.; Visticot, J. P.; Elhanine, M.; Soep, B. Prereactive Evolution of Monoalkenes Excited in the 6 eV Region. *J. Chem. Phys.* **2000**, *113*, 237–248.
- (18) Kosma, K.; Trushin, S. A.; Fuss, W.; Schmid, W. E. Ultrafast Dynamics and Coherent Oscillations in Ethylene and Ethylene-d4 Excited at 162 nm. *J. Phys. Chem. A* **2008**, *112*, 7514–7529.
- (19) Tao, H.; Allison, T. K.; Wright, T. W.; Stooke, A. M.; Khurmi, C.; van Tilborg, J.; Liu, Y.; Falcone, R. W.; Belkacem, A.; Martinez, T. J. Ultrafast Internal Conversion in Ethylene. I. The Excited State Lifetime. *J. Chem. Phys.* **2011**, *134*, 244306.
- (20) Citroni, M.; Fanetti, S.; Falsini, N.; Foggi, P.; Bini, R. Melting Dynamics of Ice in the Mesoscopic Regime. *Proc. Natl. Acad. Sci. U. S. A.* **2017**, *114*, 5935–5940.
- (21) Fanetti, F.; Falsini, N.; Bartolini, P.; Citroni, M.; Lapini, A.; Taschin, A.; Bini, R. Superheating and Homogeneous Melting Dynamics of Bulk Ice. *J. Phys. Chem. Lett.* **2019**, *10*, 4517–4522.
- (22) Scelta, D.; Ceppatelli, M.; Ballerini, R.; Hajeb, H.; Peruzzini, M.; Bini, R. Spray-Loading: A Cryogenic Deposition Method for Diamond Anvil Cell. *Rev. Sci. Instrum.* **2018**, *89*, 053903.
- (23) Bini, R.; Ballerini, R.; Pratesi, G.; Jodl, H. J. Experimental Setup for Fourier Transform Infrared Spectroscopy Studies in Condensed Matter at High Pressure and Low Temperatures. *Rev. Sci. Instrum.* **1997**, *68*, 3154–3160.
- (24) Serrano-Andrés, L.; Merchán, M.; Nebot-Gil, I.; Lindh, R.; Roos, B. O. Towards an Accurate Molecular-Orbital Theory for Excited-States: Ethene, Butadiene, and Hexatriene. *J. Chem. Phys.* **1993**, *98*, 3151–3162.
- (25) Avrami, M. Kinetics of Phase Change. I General Theory. *J. Chem. Phys.* **1939**, *7*, 1103–1112.
- (26) Avrami, M. Kinetics of Phase Change. II Transformation-Time Relations for Random Distribution of Nuclei. *J. Chem. Phys.* **1940**, *8*, 212–224.
- (27) Avrami, M. Phase Change, and Microstructure Kinetics of Phase Change. *J. Chem. Phys.* **1941**, *9*, 177–184.
- (28) Hulbert, S. F. Models for Solid-State Reactions in Powdered Compacts: A Review. *J. Br. Ceram. Soc.* **1969**, *6*, 11–20.
- (29) Gedanken, A.; Kuebler, N. A.; Robin, M. B. An MPI Search for the $\pi \rightarrow 3p$ Rydberg States of Ethylene. *J. Chem. Phys.* **1982**, *76*, 46–52.
- (30) Williams, B. A.; Cool, T. A. Two-Photon Spectroscopy of Rydberg States of Jet-Cooled C_2H_4 and C_2D_4 . *J. Chem. Phys.* **1991**, *94*, 6358–6366.
- (31) Merer, A. J.; Mulliken, R. S. Ultraviolet Spectra and Excited States of Ethylene and its Alkyl Derivatives. *Chem. Rev.* **1969**, *69*, 639–656.
- (32) Klessinger, M.; Michl, J. *Excited States and Photochemistry of Organic Molecules*; VCH: New York, 1995.
- (33) Krawczyk, R. P.; Viel, A.; Manthe, U.; Domcke, W. Photoinduced Dynamics of the Valence States of Ethene: A Six-Dimensional Potential-Energy Surface of Three Electronic States with Several Conical Intersections. *J. Chem. Phys.* **2003**, *119*, 1397–1411.
- (34) Sension, R. J.; Hudson, B. S. Vacuum Ultraviolet Resonance Raman Studies of the Excited Electronic States of Ethylene. *J. Chem. Phys.* **1989**, *90*, 1377–1389.
- (35) Mino, L.; Barzan, C.; Martino, G. A.; Piovano, A.; Spoto, G.; Zecchina, A.; Groppo, E. Photoinduced Ethylene Polymerization on the Cr^{VI}/SiO_2 Phillips Catalyst. *J. Phys. Chem. C* **2019**, *123*, 8145–8152.
- (36) Fürstner, A.; Davies, P. W. Catalytic Carbophilic Activation: Catalysis by Platinum and Gold π Acids. *Angew. Chem., Int. Ed.* **2007**, *46*, 3410–3449.
- (37) Hertwig, R. H.; Koch, W.; Schroder, D.; Schwarz, H.; Hrusak, J.; Schwerdtfeger, P. A Comparative Computational Study of Cationic Coinage Metal-Ethylene Complexes $(C_2H_4)_M^+$ ($M = Cu, Ag, Au$). *J. Phys. Chem.* **1996**, *100*, 12253–12260.
- (38) Tishchenko, O.; Li, R.; Truhlar, D. G. Metal-Organic Charge Transfer can Produce Biradical States and is Mediated by Conical Intersections. *Proc. Natl. Acad. Sci. U. S. A.* **2010**, *107*, 19139–19145.